

# Writhing Geometry of Stiff Polymers and Scattered Light

A.C. Maggs

Laboratoire de Physico-Chimie Théorique, ESPCI-CNRS, 10 rue Vauquelin, 75005 Paris, France.

12:52 14/9/2001

**Abstract.** The geometry of a smooth line is characterized *locally* by its curvature and torsion, or *globally* by its writhe. In many situations of physical interest the line is, however, not smooth so that the classical Frenet description of the geometry breaks down everywhere. One example is a thermalized stiff polymer such as DNA, where the shape of the molecule is the integral of a Brownian process. In such systems a natural frame is defined by parallel transport. In order to calculate the writhe of such non-smooth lines we study the area distributions of random walks on a sphere. A novel transposition of these results occurs in multiple light scattering where the writhe of the light path gives rise to a Berry phase recently observed in scattering experiments in colloidal suspensions.

## 1 Introduction

The classic mathematical description of the geometry of a line in three dimensional space uses a specific choice of frame, the Frenet frame [1] involving the tangent,  $\mathbf{t}$  the normal,  $\mathbf{n}$  and binormal,  $\mathbf{b}$  to the curve. However [2] this description is only valid for curves which are  $\mathcal{C}^3$ , and for which the curvature,  $\kappa$  does not vanish. Locally, by appropriate choice of axes, the shape of a three dimensional curve is approximated by the curve [3] as

$$\mathbf{r}(s) = \left( s, \frac{\kappa}{2}s^2, \frac{\kappa\tau}{6}s^3 \right) \quad (1)$$

where  $\tau$  is the torsion and  $s$  the curvilinear distance, showing, explicitly, the need for high order derivatives in order to define the torsion. In this article we show that while many problems involving elastic beams often fall within this class of smoothness the case of *non-smooth* curves is very far from being a mathematical curiosity; it is even the generic case when one is interested the *statistical mechanics* of fluctuating lines. Recent micromanipulation experiments performed on DNA molecules are one place where these considerations have been found to be important.

Very similar ideas have recently been shown to apply in multiple light scattering [4] where the tortuosity of the light path through a sample gives rise to a Berry phase. We shall show here that the theory of Berry phases in multiple scattering samples is closely related to the statistical mechanics of DNA considered as a fluctuating, stiff thread.

## 2 Intrinsic Geometry a Line

The description of the geometry based on the Frenet frame can be replaced by one based on the intrinsic geometry of

the tangent space to a curve: The unit tangent  $\mathbf{t}(s)$  to a curve lives on a sphere,  $\mathcal{S}_2$ . We now chose an arbitrary initial vector  $\mathbf{n}'(0)$ , perpendicular to  $\mathbf{t}(0)$ . Clearly any vector which is perpendicular to  $\mathbf{t}(s)$  is in the tangent space of  $\mathcal{S}_2$ , allowing a definition  $\mathbf{n}'(s)$  by parallel transport from  $\mathbf{n}'(0)$  [5]. Finally, define  $\mathbf{b}'$  to be perpendicular to both  $\mathbf{t}$  and  $\mathbf{n}'$ , forming the alternative frame. Clearly this recipe is defined for all curves for which  $\mathbf{t}(s)$  is continuous even if non-smooth.

Parallel transport about a closed loop on a sphere leads to an anholonomy. This anholonomy has been independently discovered many times in different fields of physics. Indeed Foucault's pendulum can be understood as one simple example of this phenomenon [6]. In the literature on DNA and knots following Fuller [7] and White [8] the anholonomy is known as *writhing*,  $\mathcal{W}r$ ; it was discovered as part of a topological invariant of closed ribbons, the linking number. In the quantum literature the anholonomy is the origin of the geometric phase discussed by Rytov [9] and Berry [10]. Some physical consequences are illustrated in a simple example in Figure (1). In this figure a square prism is folded into a non-planar configuration. One face of the prism is marked with a vector  $\mathbf{E}$ . We see that the bending of the prism in three dimensional space has led to a rotation of the vector  $\mathbf{E}$  about the vertical axis. We now consider the spherical curve  $\mathbf{t}(s)$  corresponding to Figure (1); application of the Gauss-Bonnet theorem to  $\mathbf{t}(s)$  allows one to calculate the angle of rotation: It is identical to the area enclosed by  $\mathbf{t}(s)$  on  $\mathcal{S}_2$ . Indeed we find that  $\mathbf{t}(s)$  encloses  $1/8$  of a sphere, corresponding to a rotation of  $\pi/4$  of the vector  $\mathbf{E}$ .

We note that for smooth lines for which  $\mathbf{t}(s)$  is a closed curve the local measure of the tortuosity of a curve,  $\tau$  and the global measure,  $\mathcal{W}r$  are linked by the equation

$$2\pi \mathcal{W}r + \int \tau ds = 0 \quad \text{mod } 2\pi. \quad (2)$$

### 3 Statistical mechanics of bending of stiff polymers

The bending energy of a stiff beam in the slender body approximation of elasticity is given by

$$E = \frac{\mathcal{K}}{2} \int \left( \frac{d\mathbf{t}(s)}{ds} \right)^2 ds, \quad (3)$$

where  $\mathcal{K}$  is the bending modulus. Such elastic descriptions are often used to describe the mechanics of stiff biopolymers. At a non-zero temperature the polymer retains memory of its orientation over a characteristic distance  $\ell_p = \mathcal{K}/k_B T$  where  $T$  is the temperature.  $\ell_p$  is known as the *persistence length*. This length should be compared with the diameter,  $d$  of the polymer. Clearly it is only when  $\ell_p/d$  is large that a continuum description in terms of an elastic line has sense. For DNA one finds  $\ell_p \sim 50nm$  and  $\ell_p/d \sim 30$ . Other stiffer biopolymers such as actin filaments are also studied in the laboratory with values of  $\ell_p/d$  as large as 2000. These filamentary systems are particularly easy to study using methods such as scanning fluorescence microscopy which allow direct measures of the three dimensional shape of the system.

To calculate the partition function one must now sum over all paths

$$\mathcal{Z} = \sum_{paths} e^{-E/k_B T} \quad (4)$$

The sum for the partition function is clearly closely related to path integrals studied in quantum mechanics. Formally the energy Eq. (3) looks like the kinetic energy of a free particle moving on a sphere. From the path integral Eq. (4) one derives a Fokker-Planck equation which is entirely analogous to the Schroedinger equation for a particle on a sphere:

$$\frac{\partial P(\mathbf{t}, s)}{\partial s} = \frac{1}{2\ell_p} \nabla^2 P(\mathbf{t}, s), \quad (5)$$

where  $\nabla^2$  is the Laplacian operator on the sphere. Here  $P(\mathbf{t}, s)$  is the probability of finding the chain oriented in the direction  $\mathbf{t}$  at the point  $s$ . As a function of  $s$  the vector  $\mathbf{t}$  “diffuses” with diffusion coefficient  $1/(2\ell_p)$ . The full distribution function of the orientational and spatial degrees of freedom for the polymer  $Q(\mathbf{r}, \mathbf{t}, s)$  is then found by noting that the shape of the polymer is found by integration of  $\mathbf{t}(s)$  so that

$$\frac{\partial Q}{\partial s} + \mathbf{t} \cdot \nabla_{\mathbf{r}} Q = \frac{1}{2\ell_p} \nabla_{\mathbf{t}}^2 Q \quad (6)$$

*i.e.* the shape evolves by convection along  $\mathbf{t}$ .

From the diffusion like Eq. (5) we understand why the torsion and the Frenet frame are not useful at non-zero temperatures: A typical configuration of a stiff polymer is the realization of an *orientational diffusion process*.  $\mathbf{t}(s)$  is continuous but not differentiable; the Frenet frame is undefined everywhere (with probability 1). Despite this low

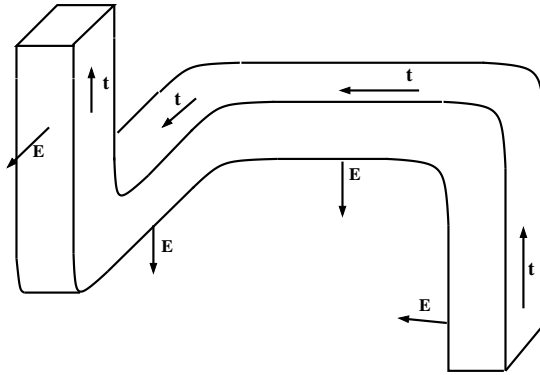


**Fig. 1.** A tortuous bar in space can represent either the shape of a fluctuating molecule such as DNA, or the path of a light beam transmitted along a fibre. The relative rotation,  $\Phi = \pi/2$ , between the two ends is an example of *writhe*,  $\mathcal{W}r$  where  $\Phi = 2\pi \mathcal{W}r$ . For light transmitted along a fibre with polarization vector  $\mathbf{E}$  this rotation is a simple example of a Berry phase.

smoothness it is possible to study the parallel transport of the vector  $\mathbf{n}'$ .

In applications in polymer physics one is interested in the magnitude of torsional fluctuations (such as shown in Figure (1)) due to the thermal fluctuations. Using the Fuller-Berry result linking anholonomy to  $\mathbf{t}(s)$  one is lead to study the distribution distribution of the area enclosed by loops by Brownian paths. This is in fact an old problem, first treated by Levy [11] in the Euclidean plane and more recently on the sphere [12]. For short chains we use Levy’s results to explicitly find the the distribution of the angle of rotation  $\Phi$  due to writhing between the ends of a filament of length  $L$  as

$$\mathcal{P}(\Phi) = \frac{\ell_p}{2L} \frac{1}{\cosh^2(\Phi \ell_p/L)} \quad (7)$$

For long chains the problem is difficult, there are ambiguities in the definition of area on the sphere, [13]. The Gauss-Bonnet theorem only allows a definition of the area mod  $4\pi$  and the more elaborate expression of Călugărean based on the Gauss linking linking number must be used to calculate the rotation angle.

### 4 Application to DNA

Very elegant experiments have been performed [15] on the mechanics of thermalized DNA molecules and interpreted with theories of fluctuating elastic threads. In these experiments a bead is attached to each end of a long molecule. The beads are held in magnetic traps which allows the simultaneous application of a force and couple. To describe these experiments theoretically one adds the force and couple into the bending energy Eq. (3). This leads to a Hamiltonian analogous to that of a particle in the presence of a Dirac monopole [16].

$$E = \frac{\mathcal{K}}{2} \int \left( \frac{d\mathbf{t}(s)}{ds} \right)^2 + f \mathbf{t} \cdot \hat{\mathbf{e}}_z + \Gamma \frac{(\hat{\mathbf{e}}_z \times \mathbf{t})}{1 + \mathbf{t} \cdot \hat{\mathbf{e}}_z} \cdot \dot{\mathbf{t}} ds, \quad (8)$$

where  $f$  is the external force pulling in the direction  $\hat{e}_z$  and  $\Gamma$  is the external torque. Experimentally one measures the mean separation of the two beads as a function of  $f$  and  $\Gamma$ . Good agreement is found with calculations based on Eq. (8). Most experiments can however be explained with a version of this Hamiltonian expanded to quadratic order in the fluctuations in  $\mathbf{t}$ , valid when the external force is larger than  $k_B T / \ell_p$  [17].

Under large forces this continuum description of DNA molecules breaks down due to an instability in the base structure of the molecule. For even higher forces the hydrogen bonds holding the two DNA strands are torn apart and the molecule is denatured. These events are clearly beyond any continuum theory and are must be treated by atomistic simulations [18].

## 5 Multiple light scattering

If one shines light into a inhomogeneous medium then the direction of propagation of the light is modified by scattering. Eventually the light gets back to the surface and re-escapes from the material. Such strongly scattering media are familiar from every day life, for instance milk, white paper or even biological tissues. One is often interested in optical imaging as deeply as possible in these materials: A particularly important application is the diagnostics of severe burns; one needs to know the degree of tissue damage as a function of depth over a large area. Empirically it is known that the quality of imaging in such media is enhanced if polarization discrimination is used to filter the light. Rather surprisingly circularly and linearly polarized light do not display the same quality and resolution in imaging. We shall now show that the statistical mechanical treatment of scattering in such media is very close to that of the stiff polymer introduced above. The idea of parallel transport will be used to understand the polarization patterns observed at the surface of samples.

In systems with weak, large scale heterogeneities, the scattering of a beam of light is largely in the forward direction, [19]. Each independent scattering event changes the direction of propagation by some small random angle. We model this process as giving rise to angular diffusion in the propagation direction of the light just as in Eq. (5). As shown in [20] the helicity of photons is conserved in forward scattering processes over a length which is larger than  $\ell_p$ . We shall thus neglect such events in the following discussion. This conservation implies that the polarization vector of linearly polarized light evolves by parallel transport on  $\mathcal{S}_2$  with  $\mathbf{t}$  the direction of propagation of the light and  $n'$  the polarization vector during the scattering process. This is exactly the condition needed for the development of a Berry or geometric phase in the scattered light.

We use these remarks to understand recent rather elegant experiments [21] performed on colloidal solutions, motivated by problems in biological imaging. In the experiments a linearly polarized light beam is focused to a point on the surface of a colloidal solution. The surface of



**Fig. 2.** False color image of polarization patterns on the surface of a beaker of a colloidal solution [21] of  $2\mu\text{m}$  latex beads. Linearly polarized light is incident at a spot at the center of the image. The surface of the beaker is imaged with a camera through a linear analyzer. The analyzer is crossed with respect to the polarization of the incident beam. We see a clear four-fold symmetry in the intensity of the backscattered light with the maximum in inclined intensity at an angle of 45 degrees to the direction of the polarizers.

the solution is then imaged through a second linear analyzer. One observes a clear pattern of brightness on the surface with fourfold symmetry about the incident beam, Figure (2)

Let us proceed by translating the backscattering geometry into an ensemble of paths on the unit sphere,  $\{\mathbf{t}\}$  in order to apply the Fuller-Berry's result. As shown in Figure (3) backscattered light corresponds to a path from the south to north poles of the sphere,  $\mathbf{t}(s)$ , describing the direction of propagation. Each path from the south to north pole is a realization of a random walk on the sphere. We take as a reference state light scattered to the left, polarized in the plane of the page. For the reference state the original polarization vector  $\mathbf{E}_A$  is parallel transported around the sphere, Figure (3, bottom) so that the initial and final vectors are antiparallel. Consider, now, a second azimuthal direction with a trajectory  $\mathbf{t}'(s)$ . This new trajectory together with the reference path form a closed loop on the sphere which allow us to apply the Berry result. As the point of observation on the sample,  $B$ , changes and winds an angle of  $2\pi$  about the incident beam,  $A$ , the new path  $\mathbf{t}'(s)$  on the sphere sweeps out a solid angle of  $4\pi$ .

Clearly in a given azimuthal direction different paths are possible with a distribution of values possible for the writhe. With an incoherent light source one must sum the intensity over all paths in a given azimuthal direction. Since these paths are correlated we deduce that the polarization at the surface of the sample rotates  $4\pi$  or *two full turns* as we move just once about the incident beam.

Since a linear analyzer is sensitive to the angle of rotation modulo  $\pi$  we see that there are four radial directions in which an analyzer detects a maximum in the intensity.

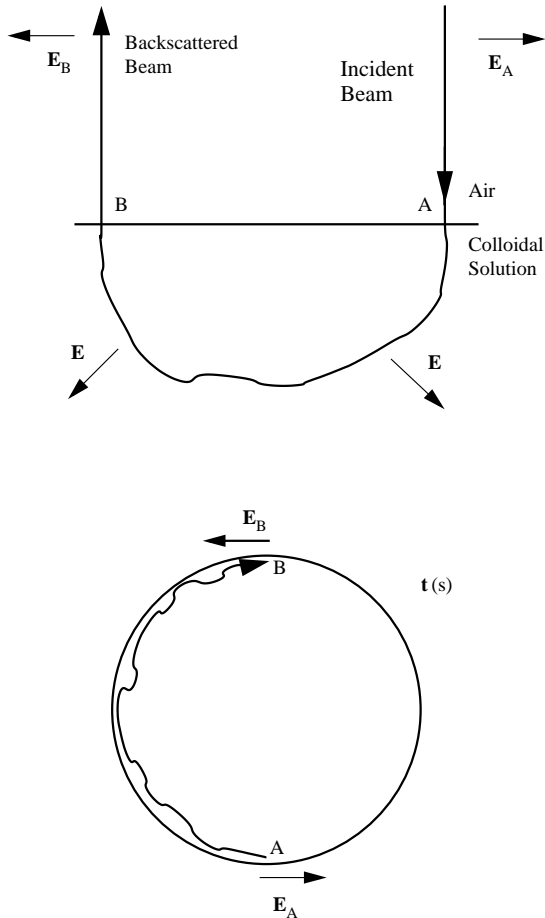


**Fig. 3.** *top:* Light is incident on a multiple scattering medium. The direction of propagation is randomly bent back and the light escapes from the surface. *bottom* The direction of propagation of the scattered light is plotted on a sphere. Incident light corresponds to the south pole,  $A$ . The escaping light corresponds to the north pole,  $B$ . The indicated path is scattered principally to the left so that on the sphere the path remains, on average on the western area of the sphere. As the point of observation goes around the incident beam, an angle of  $2\pi$ , the path between the poles sweeps out an area on the sphere of  $4\pi$ . From the results on geometric phases we deduce that the polarization also rotates  $4\pi$ .

One can now understand that the difference in the coupling of the Berry phase to linearly and circularly polarized light is partially responsible for their different imaging qualities in tissue: An object hidden deep under the surface of the beaker in Figure (2) can only weakly modify the intensity at the surface. This weak modification is easily hidden by the strong variation in intensity due to the Berry phase.

## 6 Conclusions

We have seen that two rather different physical systems are explained using simple ideas from the geometry of lines. In many physical situations a description in terms of parallel transport and intrinsic geometry is more natural than the classic description based on the Frenet Frame.

Finally we note there is subtle point that we have skipped over in the light scattering problem: The scattering cross-section of spherical particles in the Rayleigh-Gans regime decays rather slowly at large angles. The mean square scattering angle thus contains a logarithmic divergence which implies that the angular diffusion coefficient is not defined unless a cut off is introduced in the problem. In systems with smoother variations of the optical properties such as a critical fluid the scattering cross section falls off quickly and no cut off is needed. This divergence is also linked with the helicity flipping which occurs in scattering from spherical particles [20].

The image of figure (2) was kindly provided by A. H. Hielscher, Depts. of Biomedical Engineering and Radiology, Columbia University, New York, NY.

## References

1. H.S.M. Coexter, *Introduction to Geometry*, (John Wiley & Sons, 1989).
2. R.L Bishop, *American. Math. Monthly.* **82**, 246, (1975).
3. Erwin Kreyszig *Differential Geometry* (Dover, 1991).
4. A.C. Maggs, V. Rossetto. In press *Phys. Rev. Lett.*
5. A.C. Maggs *J. Chem. Phys.* **114**, 5888 (2001).
6. *Geometric phases in physics.* ed. A. Shapere, F. Wilczek. (World Scientific 1989).
7. F.B. Fuller, *Proc. Natl. Acad. Sci.* **68**, 815, (1971), *Proc. Natl. Acad. Sci* **75**, 3557, (1975).
8. J.H. White *Am. J. Math.* **91** 693 (1969).
9. S.M. Rytov, *Dokl. Akad. Nauk. USSR*, **18**, 263 (1938). Reprinted in *Topological phases in quantum theory* (World Scientific, 1989).
10. M.V. Berry, *Nature*, **326**, 277-278 (1987).
11. P. Levy, *Processus Stochastiques et Mouvement Brownien*, (Paris: Editions Jacques Gabay, 1948).
12. M. Antoine, A. Comtet, J. Desbois, S. Ouvry, *J. Phys A.* **24** 2581, (1991).
13. A.C. Maggs, V. Rossetto, Comment on [16] in press *Phys. Rev. Lett.*
14. G. Călugăreanu, *Rev. Math. Pures Appl.* **4**, 5 (1959).
15. T. R. Strick, J.-F. Allemand, D. Bensimon, A. Bensimon, and V. Croquette, *Science* **271**, 1835 (1996).
16. C. Bouchiat and M. Mézard, *Phys. Rev. Lett.* **80**, 1556, (1998).
17. P. Nelson, *Biophys. J.* **74** 2501-2503 (1998).
18. J.-F. Allemand, D. Bensimon, R. Lavery, V. Croquette. *Proc. Natl. Acad. Sci (USA)* **95**, (1998).
19. F.C. Mackintosh, J.X. Zhu, D.J. Pine, D.A. Weitz, *Phys. Rev.* **B40**, 9342-9345 (1989).
20. E.E. Gorodnichev, A.I. Kuzovlev, D.B. Rogozkin, *JETP lett.* **68**, 22-28 (1998).
21. A.H. Hielscher *et al.* *Optics exp.* **1**, 441-453 (1997).